4426 *Chem. Mater.* **2010,** *22,* 4426–4434
DOI:10.1021/cm1011026

CHEMISTRY OF MATERIALS
Article

Excimer Emission from Self-Assembly of Fluorescent Diblock Copolymer Prepared by Atom Transfer Radical Polymerization

Jungmok You,[†] Jeong Ae Yoon,[‡] Jeonghun Kim,[†] Chih-Feng Huang,[‡] Krzysztof Matyjaszewski,[‡] and Eunkyoung Kim*,[†]

[†]*Department of Chemical and Biomolecular Engineering, Yonsei University, 262 Seongsanno, Seodaemun-gu, Seoul 120-749, Korea, and* [‡]*Department of Chemistry, Carnegie Mellon University, Pittsburgh, Pennsylvania 15213*

Received April 20, 2010. Revised Manuscript Received June 17, 2010

Well-defined fluorescent copolymers of methyl methacrylate with 1-pyreneylmethyl methacrylate were synthesized by atom transfer radical polymerization (ATRP). The random and block copolymer could be clearly distinguished by their glass-transition temperature (T_g) values, with a single T_g value (124 °C) for the random polymer, and two T_g values (115 and 158 °C) for the block copolymer. The emission spectra of the copolymers were different in excimer emission, allowing analysis of the ordering of the two polymers, by determining the ratio between excimer emission (I_E) and monomer emission (I_M). The fluorescence spectra of the random copolymer exhibited both monomer and excimer emission of pyrene with a I_E/I_M ratio of 1.20−1.39 at a concentration of 0.001−0.05 mg/mL. The block copolymer exhibited strong excimer emission with an emission quantum yield for the excimer (Φ_E) of 42%. The I_E/I_M ratio from the block copolymer was >25, even in a very dilute solution. The Φ_E value increased to 68% when the block copolymer solution was processed to a thin film, indicating increased interactions among the pyrene block by self-assembly. In addition, nanopores were formed from the block copolymer, while no specific morphology was found from the random copolymer. The average diameter of the nanopores from block copolymer was ~300 nm. Upon thermal annealing of the block copolymer film, a dramatic increase in excimer emission was observed to give a high Φ_E value of 89%. A face-to-face pyrene assembly in the block copolymer was observed on the high-resolution transmission electron microscopy (HR-TEM) images, from which the average packing period of the well-defined pyrene block was estimated to range from 4.5 Å for pyrene block width to 5.6 Å for the width of PMMA mainchain.

Introduction

The investigation of ordered organic nanostructures arising from self-aggregation of chromophores is important for the academic understanding of molecular interaction, as well as potential applications including catalysis, sensors, adsorbents, scaffolds, photonics, and optoelectronics.[1−6] Noncovalent interactions such as hydrogen bonding, π-stacking, dipole−dipole interaction, and van der Waals forces produce thermodynamically ordered associations of self-organized materials including block copolymer and liquid crystals.[7−11] These self-organized nanostructures are functionalized by the attachment of optically or electronically active groups to apply them for imaging or active devices. In particular, by attaching fluorescent probes to the polymer, one can efficiently monitor self-assembly induced molecular changes in the polymer structure. Fluorescent probes have been used for monitoring conformational changes and molecular interactions in polymers, because their photophysical and photochemical properties are sensitive to environmental changes such as temperature, polarity, rigidity, and relative proximity.[12] Among fluorescent probes, pyrene has several advantages: it shows high sensitivity to its local environment and the ability to form excimers, which

*Author to whom correspondence should be addressed. E-mail: eunkim@yonsei.ac.kr.

(1) Kresge, C. T.; Leonowics, M. E.; Roth, W. J.; Vartuli, J. C.; Beck, J. S. *Nature* **1992**, *359*, 710–712.
(2) (a) Sayari, A. *Chem. Mater.* **1996**, *8*, 1840–1852. (b) Wijnhoven, J. E. G. J.; Vos, W. L. *Science* **1998**, *281*, 802–804.
(3) (a) Kim, E.; Jung, S. *Chem. Mater.* **2005**, *17*, 6381–6387. (b) Kim, E.; Kim, Y. *Mol. Cryst. Liq. Cryst.* **2006**, *447*, 173–179. (c) Kim, Y.; Kim, E. *Curr. Appl. Phys.* **2006**, *6*, e202–e205. (d) Baek, J.; Kim, Y.; Kim, E. *J. Nanosci. Nanotechnol.* **2008**, *8*, 4851–4855. (e) Kim, Y.; Yang, S. Y.; Kim, E. *J. Nanosci. Nanotechnol.* **2010**, *10*, 263–268.
(4) Imhof, A.; Pine, D. J. *Nature* **1997**, *389*, 948–951.
(5) Joannopoulos, J. D.; Villeneuve, P. R.; Fan, S. *Nature* **1997**, *386*, 143–149.
(6) Whitesides, G. M.; Mathias, J. P.; Seto, C. T. *Science* **1991**, *254*, 1312–1319.
(7) Mallia, V. A.; Tamaoki, N. *Chem. Soc. Rev.* **2004**, *33*, 76–84.
(8) Goodby, J. W.; Mehl, G. H.; Saez, I. M.; Tuffin, R. P.; Mackenzie, G.; Auzèly-Velty, R.; Benvegnu, T.; Plusquellec, D. *Chem. Commun.* **1998**, 2057–2070.
(9) Abdallah, D. J.; Weiss, R. G. *Adv. Mater.* **2000**, *12*, 1237–1247.
(10) Hanabusa, K.; Yamada, M.; Kimura, M.; Shirai, H. *Angew. Chem., Int. Ed. Engl.* **1996**, *35*, 1949–1951.
(11) Shinkai, S.; Muratab, K. *J. Mater. Chem.* **1998**, *8*, 485–495.
(12) (a) Yun, C.; You, J.; Kim, J.; Huh, J.; Kim, E. *J. Photochem. Photobiol., C* **2009**, *10*, 111–129. (b) Yoo, J.; Kwon, T.; Sarwade, B. D.; Kim, Y.; Kim, E. *Appl. Phys. Lett.* **2007**, *91*, 241107–241109. (c) Kim, Y.; Kim, E.; Clavier, G.; Audebert, P. *Chem. Commun.* **2006**, 3612–3614. (d) You, J.; Heo, J. S.; Lee, J.; Kim, H.-S.; Kim, H. O.; Kim, E. *Macromolecules* **2009**, *42*, 3326–3332.

Published on Web 07/07/2010

allows valuable information to be obtained, such as hydrodynamic volume, radius of gyration, reputation, and self-assembly in polymer physics and chemistry.[13−15] In particular, pyrene shows unique monomer and excimer emissions at considerably different wavelengths, depending on the relative proximities between pyrene molecules.[16] The pyrene excimer is sensitive to the distance between and the geometry of nearby pyrene units, and the response is ratiometric, making this a highly attractive method to probe chemical or biological interactions.[17] By designing diblock copolymers with pyrene block, we may explore self-assembly of fluorescent diblock copolymers (BCPs) to generate ordered microdomains driven thermodynamically by microphase separation, as recently discussed for many BCPs.[18] These BCP microdomain structures can be used as templates for integrated circuits, filters, plasmonic and photonic bandgap structures, catalysts, templates, sensors, and solar cells.[19−27]

Here, we describe the synthesis and self-association properties of diblock copolymers with a pendant pyrene unit via atom transfer radical polymerization (ATRP).[28] Controlled/living radical polymerization[29] by ATRP allowed us to precisely control the length and distribution of pyrene units in polymer chains. In contrast to previous reports, the objective of this paper was to directly study the influence of the distribution of pyrenes in random versus block copolymers. Also unlike previous studies of BCPs, the current approach enables us to synthesize block copolymers with a fluorescent probe with low polydispersity in molecular weights. For pyrene, in particular, spatial restriction is known to influence excimer formation, but quantitative statements are rare. We explored a dramatic increase in excimer emission and generated ordered nanodomains by self-assembly of the pyrene-attached copolymer.

Experimental Section

Materials. Methyl methacrylate (99%) was obtained from Aldrich Chemicals and was passed through a column of basic alumina and then distilled prior to polymerization. Pyrene, 1-pyrenemethanol, triethylamine, anisole, methacryloyl chloride, Cu(I)Br, $CuBr_2$, Cu(I)Cl, $CuCl_2$, *N,N,N′,N″,N″*-pentamethyldiethylenetriamine (PMDETA, 99%),[30] and ethyl 2-bromo isobutyrate (EBiB) were obtained from Aldrich Chemicals and used as received.

Instruments. Molecular weights and polydispersities were determined by gel permeation chromatography (GPC). The GPC was conducted with a Waters Model 515 pump and Waters Model 410 differential refractometer using PSS columns (Styrogel with diameters of 105, 103, 102 Å) in tetrahydrofuran (THF) as an eluent at a flow rate of 1 mL/min (35 °C). Poly(methyl methacrylate) (PMMA) was used as a calibration standard, employing WinGPC software from Polymer Standards Service. ^{1}H NMR spectra were obtained using a Bruker 300 MHz spectrometer. FT-IR spectra were obtained using a TENSOR 37 (Bruker). UV spectra were obtained from a Guided Wave model 260 (Guided Wave, Inc., USA), and fluorescence was measured with a luminescence spectrometer (Perkin−Elmer, Model LS55). Differential scanning calorimetry (DSC) measurements were performed on a Netzsch/DSC 200 F3 at a heating rate of 10 °C/min under a nitrogen atmosphere. Samples were placed in an aluminum pen, sealed tightly, and scanned from 20 °C to 300 °C. Scanning electron microscopy (SEM) images were obtained with a field-emission scanning electron microscope (FE-SEM) system (Hitachi, Model S-4200). Transmission electron microscopy (TEM) images were taken using an energy-filtering transmission electron microscopy system (Carl Zeiss, Model LIBRA 120) and a high-resolution transmission electron microscopy (HR-TEM) system (JEOL, Model JEM-3010). The fluorescent films were examined using a digital camera (Canon Power Shot A640).

Sample Preparation. Polymer thin films were prepared by spin-coating on silicon wafers, carbon-coated TEM grids, and slide glasses for SEM, TEM, and fluorescence measurements, respectively. Film thickness was controlled by changing spinning speeds and concentrations of the copolymer solutions. Block copolymer films were annealed under vacuum at 60, 100, 130, and 160 °C. The specimens were slowly cooled to room temperature in air or quickly cooled to room temperature using liquid nitrogen. For TEM measurement, the specimens were stained by exposing them to osmium tetroxide (OsO_4) vapor for 2 h. Since OsO_4 reacts preferentially with the unsaturated carbon double bonds of pyrene, the stained pyrene phase appears dark in a bright-field TEM micrograph.[31]

Synthesis of 1-Pyrenemethyl Methacrylate (*PY, **1***). Monomer **1** was synthesized according to a previously reported procedure

(13) Oh, H.; Kim, J.; Kim, E. *Macromolecules* **2008**, *41*, 7160–7165.
(14) (a) Nishizawa, S.; Kato, Y.; Teramae, N. *J. Am. Chem. Soc.* **1999**, *121*, 9463–9464. (b) Sahoo, D.; Narayanaswami, V.; Kay, C. M.; Ryan, R. O. *Biochemistry* **2000**, *39*, 6594–6601.
(15) (a) Gao, H.; Matyjaszewski, K. *Macromolecules* **2007**, *40*, 399–401. (b) Oh, J. K.; Drumright, R.; Siegwart, D. J.; Matyjaszewski, K. *Prog. Polym. Sci.* **2008**, *33*, 448–477. (c) Zhang, M.; Duhamel, J. *Macromolecules* **2007**, *40*, 661–669. (d) Baker, L. A.; Crooks, R. M. *Macromolecules* **2000**, *33*, 9034–9039. (e) Kanagalingam, S.; Ngan, C. F.; Duhamel, J. *Macromolecules* **2002**, *35*, 8560–8570. (f) Im, M. J.; Park, C.; Kim, C. *Macromol. Res.* **2009**, *17*, 62–66.
(16) Winnik, F. M. *Chem. Rev.* **1993**, *93*, 587–614.
(17) (a) Oh, K. J.; Cash, K. J.; Plaxco, K. W. *J. Am. Chem. Soc.* **2006**, *128*, 14018–14019. (b) Paris, P. L.; Langenhan, J. M.; Kool, E. T. *Nucleic Acids Res.* **1998**, *26*, 3789–3793. (c) Krosky, D. J.; Song, F.; Stivers, J. T. *Biochemistry* **2005**, *44*, 5949–5959.
(18) (a) Stefik, M.; Mahajan, S.; Sai, H.; Epps, T. H., III; Bates, F. S.; Gruner, S. M.; DiSalvo, F. J.; Wiesner, U. *Chem. Mater.* **2009**, *21*, 5466–5473. (b) Wang, J.; Müller, M. *Langmuir* **2010**, *26*, 1291–1303.
(19) Raman, N. K.; Anderson, M. T.; Brinker, C. J. *Chem. Mater.* **1996**, *8*, 1682–1701.
(20) Lin, V. S. Y.; Motesharei, K.; Dancil, K. P. S.; Sailor, M. J.; Ghadiri, M. R. *Science* **1997**, *278*, 840–843.
(21) Dancil, K. P. S.; Greiner, D. P.; Sailor, M. J. *J. Am. Chem. Soc.* **1999**, *121*, 7925–7930.
(22) Ying, J. Y.; Mehnert, C. P.; Wong, M. S. *Angew. Chem, Int. Ed.* **1999**, *38*, 56–77.
(23) Hara, K.; Horiguchi, T.; Kinoshita, T.; Sayama, K.; Sugihara, H.; Arakawa, H. *Sol. Energy Mater. Sol. Cells* **2000**, *64*, 115–134.
(24) Seo, J. S.; Whang, D.; Lee, H.; Jun, S. I.; Oh, J.; Jeon, Y. J.; Kim, K. *Nature* **2000**, *404*, 982–986.
(25) Jiang, P.; Bertone, J. F.; Colvin, V. L. *Science* **2001**, *291*, 453–457.
(26) Wang, Z. S.; Huang, C. H.; Huang, Y. Y.; Hou, Y. J.; Xie, P. H.; Zhang, B. W.; Cheng, H. M. *Chem. Mater.* **2001**, *13*, 678–682.
(27) Niwa, S.; Eswaramoorthy, M.; Nair, J.; Raj, A.; Itoh, N.; Shoji, H.; Namba, T.; Mizukami, F. *Science* **2002**, *295*, 102–105.
(28) (a) Wang, J.-S.; Matyjaszewski, K. *J. Am. Chem. Soc.* **1995**, *117*, 5614–5615. (b) Wang, J.-S.; Matyjaszewski, K. *Macromolecules* **1995**, *28*, 7901–7910. (c) Matyjaszewski, K.; Xia, J. *Chem. Rev.* **2001**, *101*, 2921–2990. (d) Tsarevsky, N. V.; Matyjaszewski, K. *Chem. Rev.* **2007**, *107*, 2270–2299. (e) Matyjaszewski, K.; Tsarevsky, N. V. *Nature Chem.* **2009**, *1*, 276–288.
(29) Braunecker, W. A.; Matyjaszewski, K. *Prog. Polym. Sci.* **2007**, *32*, 93–146.
(30) Pintauer, T.; Matyjaszewski, K. *Coord. Chem. Rev.* **2005**, *249*, 1155–1184.
(31) Oeda, Y.; Nishi, O.; Matsushima, Y.; Mizuno, K.; Matsui, A. H.; Michinomae, M.; Takeshima, M.; Goto, T. *Chem. Phys.* **1996**, *213*, 421–427.

with a slight modification.[32] 1-Pyrenemethanol (5 g; 0.022 mol) was added to a solution of triethylamine (9.0 mL; 0.065 mol) in 250 mL of anhydrous methylene chloride (MC). Methacryloyl chloride (6.3 mL; 0.065 mol) was added to the solution containing 1-pyrenemethanol dropwise under stirring at 0 °C. The reaction was then conducted at room temperature overnight. The precipitates from the reaction mixture were filtered off and the solvent was evaporated to yield monomer **1** as a solid, which was recrystallized from 95% ethanol at 40 °C (yield = 90%). The spectral data were well-matched to the reported value:[33] ^{1}H NMR ($CDCl_3$), δ ppm: 7.99−8.19 (m, 9H, aromatic H), 6.15 (s, 1H, CH_2=C), 5.89 (s, 2H, CH_2O), 5.56 (s, 1H, CH_2=C), 1.97 (s, 3H, CH_3), FT-IR (cm^{-1}): 1728 (C=O stretching), 1660 (C=C stretching), 842 (pyrene ring deformation) (see Figures S1 and S2 in the Supporting Information).

Synthesis of PMMA Macroinitiator (***3***). $CuCl_2$ (3.8 mg, 0.028 mmol), PMDETA (0.045 mL, 0.022 mmol), and methyl methacrylate (3 mL, 0.028 mol) were mixed in 3 mL of anisole. The mixture was degassed by three freeze−pump−thaw cycles. Then, Cu(I)Cl (0.019 g, 0.188 mmol), with EBiB as an initiator (0.028 mL, 0.188 mmol), were added to the frozen mixture under nitrogen flow. The mixture was degassed once again, back-filled with nitrogen, and sealed under nitrogen flow. The mixture was placed in a preheated oil bath (60 °C) for 3 h. After exposing the reaction mixture to the air and diluting with THF, the solution was passed through a neutral Al_2O_3 column with THF as an eluent to remove the catalyst. The light yellow filtrate was concentrated under reduced pressure and reprecipitated into methanol. The PMMA macroinitiator precipitate was collected by filtration and dried under vacuum. The yield was 60% [M_n (GPC) = 28 900; M_w/M_n = 1.10 (GPC)]. This PMMA was used as a macroinitiator. The spectral data were well-matched to the reported FT-IR (cm^{-1}) values:[34] 2951 (C−H stretching), 1728 (C=O stretching), 1444 (CH_3 stretching), 1147 (−O−CH_3 stretching) (see Figure S1 in the Supporting Information).

Synthesis of Random Copolymer (***4***). A solution of $CuBr_2$ (4.4 mg, 0.02 mmol (using significant digits)), PMDETA (0.07 mL, 0.33 mmol), methyl methacrylate (1.26 mL, 0.012 mol), and PY (**1**) (0.4 g, 1.32 mmol) in 1.5 mL anisole was prepared. The mixture was degassed by three freeze−pump−thaw cycles. Then, Cu(I)Br (0.019 g, 0.188 mmol), with EBiB as an initiator (0.019 mL, 0.13 mmol), were added to the frozen mixture under nitrogen flow. The mixture was degassed once again, back-filled with nitrogen, and sealed under nitrogen flow. The mixture was placed in a preheated oil bath (70 °C) for 1 h. After quenching the polymerization by exposure to air and dilution with THF, the solution was passed through a neutral Al_2O_3 column with THF as the eluent to remove the catalyst. The light yellow filtrate was concentrated under reduced pressure and reprecipitated from ether. The random copolymer was collected by filtration and dried under vacuum (M_n (GPC) = 21 000; M_w/M_n = 1.3 (GPC)). This sample was denoted as P(MMA_{148}-*r*-PY_{20}), where the two numbers indicate the numbers of MMA and PY units, respectively (^{1}H NMR ($CDCl_3$), δ ppm: 7.99−8.19 (aromatic H), 5.89 (CH_2O), 3.4−0−3.60 (OCH_3), 1.75−2.0 (CH_3), 0.75−1.10 (CH_2)) (see Figure S2 in the Supporting Information).

Synthesis of Diblock Copolymer (***5***). As an example, $CuBr_2$ (0.45 mg, 0.002 mmol), PMDETA (0.003 mL, 0.015 mmol), PMMA macroinitiator (**3**) (0.388 g, 0.013 mmol) and PY (**1**) (0.2 g, 0.66 mmol) were mixed in 2 mL of anisole. The mixture was degassed three times using the freeze−pump−thaw cycle. Then, Cu(I)Br (0.0019 g, 0.013 mmol) was added to the frozen mixture under nitrogen flow. The mixture was degassed once again, back-filled with nitrogen, and sealed under nitrogen flow. The mixture was placed in a preheated oil bath (90 °C) for 24 h and quenched. The quenched solution was passed through a neutral Al_2O_3 column with THF as an eluent to remove the catalyst. The light yellow filtrate was concentrated under reduced pressure and reprecipitated from ether. The diblock copolymer was collected by filtration and dried under vacuum M_n (NMR) = 48 200; M_w/M_n = 1.23 (GPC)). The repeating unit of PMMA and PY was calculated with the GPC result (PMMA standard) and the integration of protons in the NMR result, respectively. This sample is denoted as $PMMA_{289}$-*b*-PPY_{65}, where the two numbers indicate the numbers of MMA and PY units, respectively.

(^{1}H NMR ($CDCl_3$), δ ppm: 7.30−7.90 (aromatic H), 5.00−5.40 (CH_2O), 3.50−3.70 (OCH_3), 1.75−2.0 (CH_3), 0.60−1.0 (CH_2), FT-IR (cm^{-1}): 2951 (C−H stretching), 1728 (C=O stretching), 1444 (CH_3 stretching), 1147 (−O−CH_3 stretching), 842 (pyrene ring deformation). See Figures S1 and S2 in the Supporting Information.)

Result

Synthesis and Characterization. Well-defined fluorescent diblock and random copolymers were synthesized by ATRP of methyl methacrylate (MMA) and 1-pyrenylmethyl methacrylate (PY). Scheme 1 shows the synthetic routes of PY (**1**) used as a monomer,[32] poly(methyl methacrylate) (PMMA) as a macroinitiator (**3**), pyrene-containing random copolymer (**4**), and pyrene-containing block copolymer (**5**). To synthesize pyrene-containing diblock copolymer, PMMA macroinitiator with M_n = 28 900, corresponding to 289 MMA units, was prepared first. Block extension of the PMMA macroinitiator with PY through ATRP then was conducted to yield pyrene-containing diblock copolymer (**5**).

The chemical structures of the monomer, random copolymer, and diblock copolymer were confirmed by FT-IR and ^{1}H NMR (see Figures S1 and S2 in the Supporting Information). The polymerization was also confirmed by the disappearance of the C=C vibronic peaks of methacrylate at 1660 and 830 cm^{-1} (see Figure S1 in the Supporting Information) in FT-IR spectra, as well as the proton peaks of methacrylate at 6.14 and 5.50 ppm in ^{1}H NMR (see Figure S2 in the Supporting Information). In addition, the FT-IR of the block copolymer (**5**) showed a new peak at 842 cm^{-1} after block extension. As the peak is a characteristic peak of pyrene rings, the successful formation of pyrene block extension in **5** could be confirmed. The pyrenyl protons of the block copolymer were shifted by 0.50 ppm, compared to that of the monomer and **4**, probably due to the strong interaction between tightly packed pyrenyl groups in **5**. The PMMA macroinitiator and

(32) (a) Kim, J.; Kim, Y.; Kim, E. *Macromol. Res.* **2009**, *17*, 791–796. (b) Kim, J.; You, J.; Kim, E. *Macromolecules* **2010**, *43*, 2322–2327. (c) Kim, J.; Oh, H.; Kim, E. *J. Mater. Chem.* **2008**, *18*, 4762–4768. (d) Lou, X.; Daussin, R.; Cuenot, S.; Duwez, A.-S.; Pagnoulle, C.; Detrembleur, C.; Bailly, C.; Jérôme, R. *Chem. Mater.* **2004**, *16*, 4005–4011.

(33) (a) Jiang, J.; Tong, X.; Zhao, Y. *J. Am. Chem. Soc.* **2005**, *127*, 8290–8291. (b) Choi, I. H.; Park, M.; Lee, S.-S.; Hong, S. C. *Eur. Polym. J.* **2008**, *44*, 3087–3095.

(34) Ramesh, S.; Leen, K. H.; Kumutha, K.; Arof, A. K. *Spectrochim. Acta, Part A* **2007**, *66*, 1237–1242.

Scheme 1. Synthesis of Pyrene-Containing Random Copolymer (4) and Block Copolymer (5) via ATRP, Using the Initiators 2 and 3

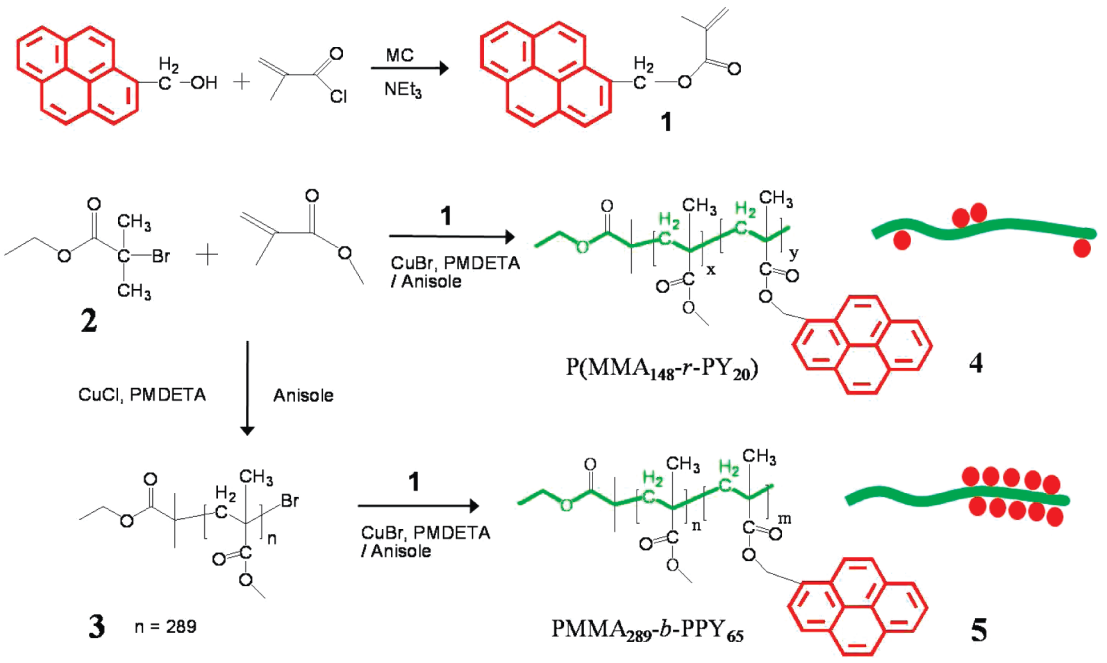

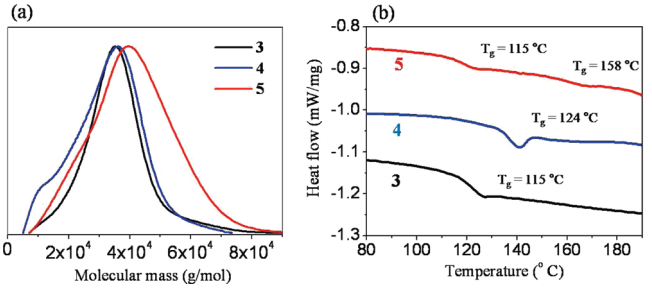

Figure 1. (a) GPC traces and (b) DSC thermograms of PMMA macroinitiator (**3**), P(MMA$_{148}$-*r*-PY$_{20}$) (**4**), and PMMA$_{289}$-*b*-PPY$_{65}$ (**5**).

pyrene-containing block copolymer were characterized by GPC, which was calibrated with PMMA standards. The pyrene content of the copolymer (λPy) was obtained as 20 and 65 for **4** and **5**, respectively, by GPC and ^{1}H NMR analysis. Thus, the random (**4**) and diblock (**5**) copolymer could be described as P(MMA$_{148}$-*r*-PY$_{20}$) and PMMA$_{289}$-*b*-PPY$_{65}$, respectively. The M_n increase of the block copolymer (**5**) was well-matched to the M_n of PMMA macroinitiator (**3**) plus M_n of PPY block (see Figure 1a). Differential scanning calorimetry (DSC) analysis for **5** showed two glass-transition temperature (T_g) values, at 115 and 158 °C, corresponding to the T_g values of the PMMA and PPY blocks, respectively, while the random polymer showed a single T_g value at 124 °C (Figure 1b). This result also confirms the formation of a diblock copolymer consisting of PMMA and PPY blocks.

Optical properties. Figure 2a shows UV−vis and photoluminescence (PL) spectra of the chloroform solutions of pyrene, **4**, and **5**. The absorption spectra of pyrene showed the characteristic three vibronic bands at 308, 321, and 336 nm. Compared to pyrene, UV absorption with the three vibronic bands for the random (**4**) and block copolymer (**5**) in solution was red-shifted by ~7 and 10 nm, respectively, possibly due to the enhanced interactions between the pyrenyl units in the copolymers.[16] The PL spectrum of **4** exhibited emission bands of not only pyrene monomer at 377, 386, and 397 nm, but also pyrene excimer at ~485 nm, as similarly observed with a highly concentrated pyrene solution.[35] On the other hand, the PL spectrum of the block copolymer (**5**) showed a strong excimer emission at 485 nm, with a negligible monomer emission, even at a low concentration. The quantum yield (Φ_E) of the block copolymer for the excimer emission was 42%, as referenced to anthracene in ethanol solution (29%). The Φ_E values of the random copolymer (**4**) and pyrene were much lower than that of **5** (16% and 11%, respectively). This clear difference between the random copolymer and the block copolymer for excimer emission arose from the different distribution of the pyrenes. In the block polymer, pyrene molecules are brought into close proximity within blocks to allow strong $\pi-\pi$ interactions, leading to only excimer emission.[36] However, the random copolymer contained both isolated pyrene units, separated by several methacrylate units, and group of pyrenes, where pyrene molecules are bonded closely to show both monomer and excimer emission.

The dependence of the pyrene distribution in the copolymer on excimer equilibrium was determined by examining the fluorescence of the excimer to monomer emission (I_E/I_M) (determined by the intensities of the excimer emission at its maximum at 485 nm and that of the pyrene at 397 nm). Generally, excimer formations are facilitated by increasing concentration of polymer, because it allows not only intramolecular but also intermolecular interaction between pyrene units. Figures 2b and 2c show the emission

(35) Birks, J. B. In *Photophysics of Aromatic Molecules*; Wiley Interscience: New York, 1970; p 302.
(36) Deepak, V. D.; Asha, S. K. *J. Phys. Chem. B* **2009**, *113*, 11887–11897.

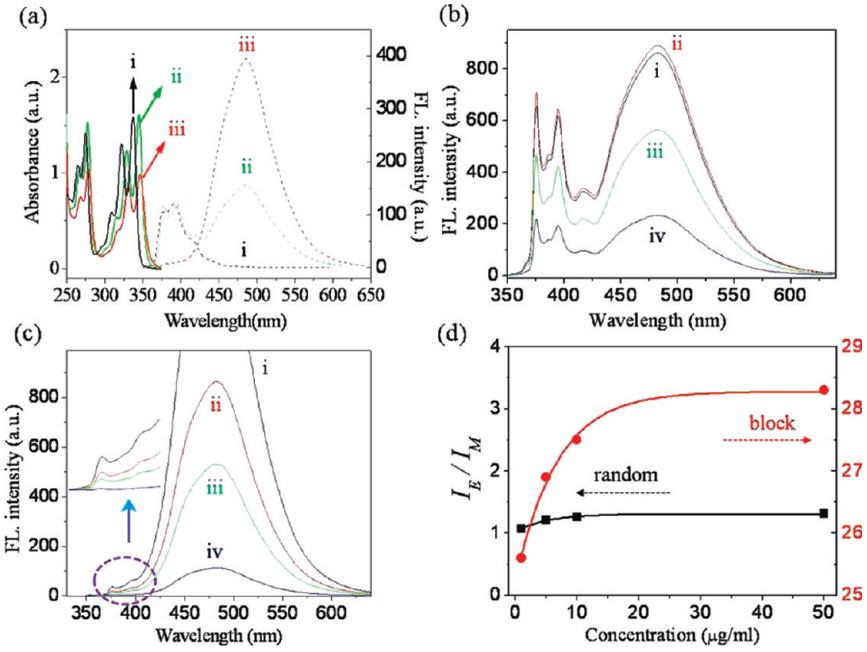

Figure 2. (a) UV−vis (solid line) and emission spectra (dotted line) of (i) pyrene (4.9×10^{-5} M), (ii) **4** (0.05 mg mL^{-1}), and (iii) **5** (0.05 mg mL^{-1}), in chloroform solution (λ_{exc} = 330 nm). (b) Emission spectra of **4** in THF solution at different concentrations ((i) 0.05. (ii) 0.01, (iii) 0.005, and (iv) 0.001 mg mL^{-1}). (c) Emission spectra of **5** in THF solution at different concentrations ((i) 0.05. (ii) 0.01, (iii) 0.005, and (iv) 0.001 mg mL^{-1}). (d) Plot of I_E/I_M against polymer concentration for **4** (denoted by solid black squares) and **5** (denoted by solid red circles).

spectra of **4** and **5** in THF solution at different concentrations. The ratio of I_E/I_M gradually increased from 1.20 to 1.39 as the concentration of **4** was increased from 0.001 mg mL^{-1} to 0.05 mg mL^{-1}. This result indicates that pyrenes interact closely in a highly concentrated solution.[36] Compared to the random copolymer, the block copolymer **5** showed strong excimer emission with a large I_E/I_M ratio of 25−29 in the concentration range of 0.001−0.05 mg mL^{-1} (see Figure 2d), because the block copolymer contains tightly packed pyrenyl groups, and the block copolymer is probably more rigid and less soluble, with a tendency toward pyrene aggregation in the solution. This result indicates that the efficiency of the excimer formation in **5** is much higher than that in **4**.

Such a large difference in excimer emission between **4** and **5** was also shown in the film state. Thin films of the block copolymer (**5**) and the random copolymer (**4**) were prepared by spin of the polymer solutions (20, 10, 5, 2.5 mg/mL in THF). Figure 3 compares the emission spectra for the spin-coated films of **4** (Figure 3a) and **5** (Figure 3b), with different thicknesses.

The overall shape of the fluorescence spectra of the copolymers was not dependent on the polymer film thickness or comparable to that in solution spectra of Figure 2. However, it was noteworthy that the emission spectra for copolymer films were slightly blue-shifted compared to those determined in solution, as shown in Figure 3c for **5**. This may be attributed to the self-aggregation of pyrene units in solid media. As the film thickened, the ratio became higher, favoring excimer formation. Such increased I_E/I_M values are observed when a fluorophore is in the film, because of increased interaction among the fluorophores in solid media. Interestingly, the I_E/I_M ratio was decreased in the film of **5** and the ratio was smaller as the film became thinner. The I_E/I_M ratio from solution and solid spectra were estimated by normalizing the fluorescence spectrum at the emission peak (Figure 3c as an example for **5**), which was increased to 25.6−28.3 in the solution of **5** (see Figure 2d). This is evident from the results in Figure 3c, where the monomer fluorescence is seen to increase more in a 30-nm-thick film than in a 230-nm-thick film of **5**. With the 30-nm-thick film, the I_E/I_M ratio was 6.5, which is ~2 times lower than that in the 230-nm-thick film.

The overall plot of the I_E/I_M ratio versus film thickness in Figure 3d is similar to a typical isotherm curve, indicating that the thickness effect could be described by a two-state model. In the general case, the fluorescence spectrum of a fluorophore does not depend on polymer film thickness.[37] Thus, the change in the I_E/I_M ratio indicates a change in the nanocale confinement on pyrene−pyrene interactions in thin films.[38] For excimer formation, a laterally packed structure would be more favorable than a perpendicular structure. However, the hydrophilic PMMA-blocks could interact first with the hydrophilic glass surface and may grow in a perpendicular geometry in the early stage of film formation.[39] In a perpendicular geometry, the pyrene−pyrene assembly is unfavorable and excimer emission is weak. As the film becomes thicker, the self-assembly between the pyrene blocks could drive the structure toward a lateral one to enhance excimer emission, as shown in Figure S3 in the Supporting Information.

Because the block copolymer emits exclusively excimer emission in solution, it can form unique self-assembled

(37) Hall, D. B.; Miller, R. D.; Torkelson, J. M. *J. Polym. Sci., Part B: Polym. Phys.* **1997**, *35*, 2795–2802.
(38) Kim, S. D.; Torkelso, J. M. *Macromolecules* **2002**, *35*, 5943–5952.
(39) Park, I.; Park, S.; Park, H.-W.; Chang, T.; Yang, H.; Ryu, C. Y. *Macromolecules* **2006**, *39*, 315–318.

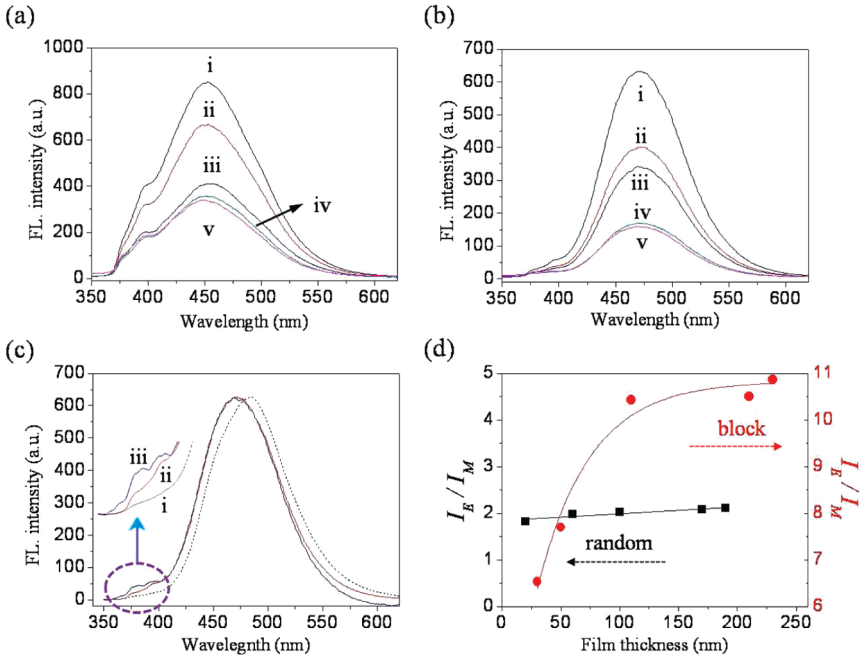

Figure 3. Emission spectra for the spin-coated film of (a) **4** with different thicknesses ((i) 190, (ii) 170, (iii) 100, (iv) 60, (v) 20 nm) and (b) **5** with different thicknesses ((i) 230, (ii) 210, (iii) 110, (iv) 50, (v) 30 nm). (c) Normalized plot of the emission spectra for **5** ((i) in chloroform solution (0.05 mg/mL), (ii) thick film with 230 nm, and (iii) thin film with 30 nm). (d) Plot of I_E/I_M ratio versus film thickness for **4** (denoted by solid black squares) and **5** (denoted by solid red circles).

structures under solid-state conditions (film). Thin films of the block copolymer (**5**) and the random copolymer (**4**) were prepared via drop casting of the polymer solutions (5 mg/mL in THF). The random copolymer film exhibited no ordered structures, as shown in Figure 4b and was transparent. Interestingly, the block copolymer films were hazy and had nanopores ~300 nm in size (see Figure 4a). Such a dramatic difference between the random and block copolymers in nanopore formation may be due to the self-assembly of the pyrene units in the block copolymer. This result is well-matched to the strong excimer emission from **5**, shown in Figures 2 and 3. The mechanism on the formation of pore morphology can be speculated based on solvent-induced breath figure formation as follows. The diblock copolymer assumes the form of a disordered phase in dilute solution upon casting. As the solvent evaporation proceeds and also temperature drops upon solvent evaporation, the diblock copolymers will tend to form spherical micelles, consisting of a core and a corona (possibly of the hydrophobic pyrene blocks). At some concentration, interaction between micelles will force a disorder−order transition, resulting in freezing of micelles in some superlattice.[40] After subsequent evaporation of the solvent, polymer films with an ordered micropore pattern could be formed because the solvent within the leaving gaps is vomited out. A continuous matrix consisting of core−corona micelles may change the shape, because of the internal pressure during solvent evaporation,

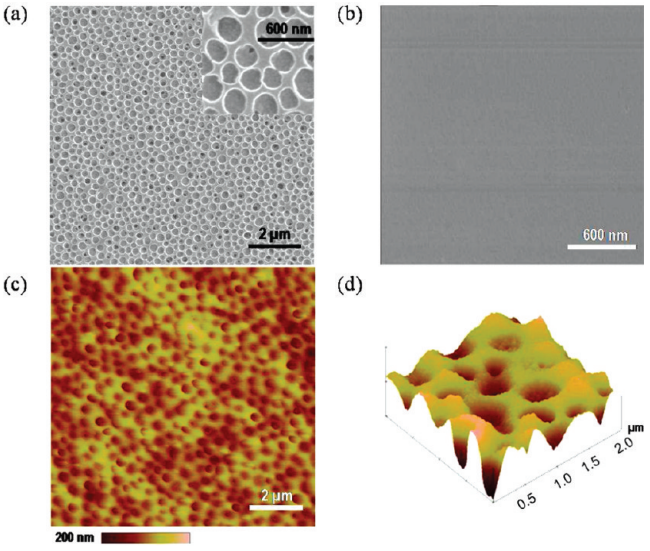

Figure 4. (a) SEM images of the film of **5** prepared by drop casting onto a silicon wafer. (Inset: magnified image). (b) SEM images of the film of **4** prepared by drop casting under the same conditions as those given for panel (a). (c and d) AFM images of the film of **5** prepared by drop casting under the same conditions as those given for panel (a) (panel (c) shows a two-dimensional image, whereas panel (d) shows a three-dimensional (3D) image).

and the pore sizes may very possibly controlled by micelle sizes, i.e., M_n of diblock copolymers, as discussed in several papers.[41] The understanding on the pore formation for the diblock copolymer should be important and thus the mechanism will be elucidated in the near future.

Figures 4c and 4d show AFM images of the block copolymer film showing a pore size of ~300 nm, which is in good agreement with morphology estimated from the SEM images in Figure 4a.

(40) (a) Ishizu, K.; Sugita, M.; Kotsubo, H.; Saito, R. *J. Colloid Interface Sci.* **1995**, *169*, 456. (b) Ishizu, K.; Tokuno, Y.; Makino, M. *Macromolecules* **2007**, *40*, 763–765.
(41) (a) Srinivasarao, M.; Collings, D.; Philips, A.; Patel, S. *Science* **2001**, *292*, 79–83. (b) Yabu, H.; Shimomura, M. *Chem. Mater.* **2005**, *17*, 5231–5234.

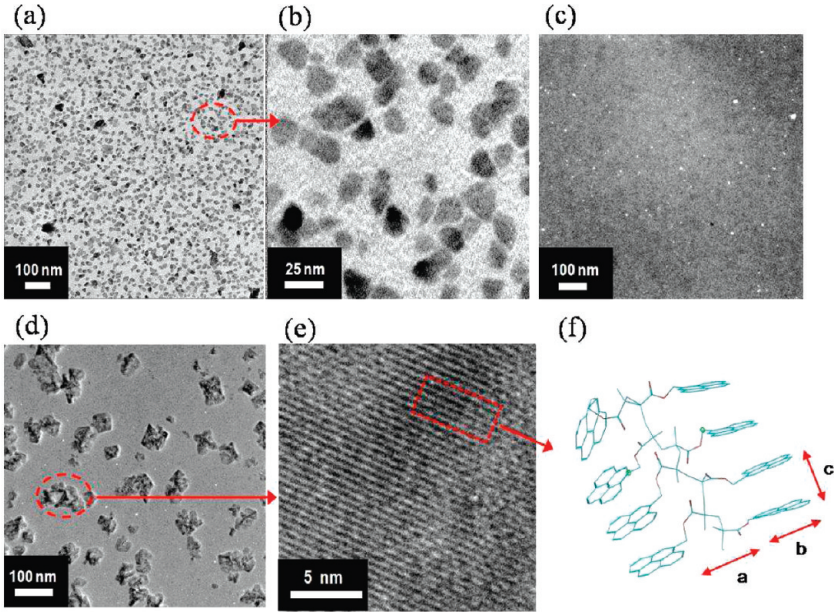

Figure 5. TEM images of (a) the film of **5** prepared from low-concentration solution (2.5 mg/mL in THF), (b) magnified image of panel (a), (c) the film of **4** prepared from low-concentration solution (2.5 mg/mL in THF), (d) the film of **5** prepared from high-concentration solution (10 mg/mL in THF). Also shown are (e) magnified images of the aggregates shown in panel (d) and (f) the proposed structure of **5** in self-assembly after thermal annealing at 160 °C.

After thermal annealing at 160 °C for 2 days, which was above the T_g value for both PMMA block and PPY blocks and then slowly cooled to room temperature, aggregates of the block copolymers gradually appeared, as a result of self-assembly. The TEM images in Figures 5a and 5b show a dark region corresponding to the stained PPY block dispersed in a lighter matrix of PMMA. The sizes of the pyrene aggregations were ~8−15 nm in the film of **5** prepared from the polymer solution of 2.5 mg/mL. Compared to the film of **5**, the random copolymer film from **4**, prepared under the same conditions as the film of **5**, did not show any dark phase (see Figure 5c), which indicates there is no pyrene aggregation. The size of the pyrene association was controlled by changing the concentration of the block copolymer solution. Figure 5d shows a much-larger pyrene association (40−100 nm in size), produced using a high-concentration polymer solution (10 mg/mL) rather than a low-concentration polymer solution (2.5 mg/mL) (see Figure 5a). The highly magnified image in Figure 5e shows alternating dark and bright lines, with average line widths of ~4.5 Å and 5.6 Å for the dark and bright lines. The face-to-face pyrene stack distance (*c* in Figure 5f) is determined as 3.2 Å, which matched well to the reported value of ~3.18−3.49 Å.[42] Thus, the bright lines may be ascribed to the separation distance between well-ordered pyrene stacks (*a* in Figure 5f), corresponding to the width of PMMA mainchain. The dark lines then could be assigned to the pyrene block width, given as *b* in Figure 5f.

This result promises nanoprocessability of the fluorescent diblock copolymer to generate finely tuned nanostructures by simple methods including solvent and thermal annealing that are applied in conventional BCPs. The effect of thermal annealing on the degree of pyrene aggregation was confirmed by emission spectra. Figure 6a shows the emission spectra of the block copolymer film before and after annealing at 60, 100, 130, and 160 °C for 2 days. The emission band of the block copolymer in the solid state (film) was observed at 470 nm.

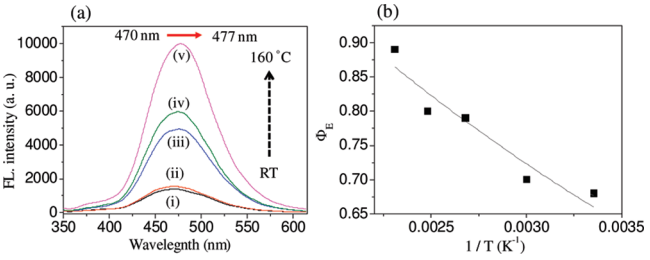

Figure 6. (a) Fluorescence spectra of the film of **5** before (i) and after thermal annealing at different temperatures, (ii) 60 °C, (iii) 100 °C, (iv) 130 °C, and (v) 160 °C, followed by slow cooling. (b) Plot of Φ_E against thermal annealing temperature.

After the block copolymer film was annealed at 60 °C, below the T_g value of the polymer, and then slowly cooled to room temperature, the intensity of the pyrene excimer emission was similar to that measured before annealing. However, when the block copolymer film was annealed at 160 °C, which is above T_g, and then slowly cooled to room temperature, the intensity of the pyrene excimer emission was significantly increased (~10 times more than the value before annealing). In addition, the emission wavelength was red-shifted to 477 nm.

These observations may be explained by the formation of aggregates between pyrene units. After the block copolymers were annealed at an elevated temperature, such aggregation was enhanced and there were further changes in the emission spectra. The pyrene excimer is very sensitive to the distance between and the geometry of two close pyrene units. The plot of Φ_E against annealing

(42) Lee, S.; Chen, B.; Fredrickson, D. C.; DiSalvo, F. J.; Lobkovsky, E.; Adams, J. A. *Chem. Mater.* **2003**, *15*, 1420–1433.

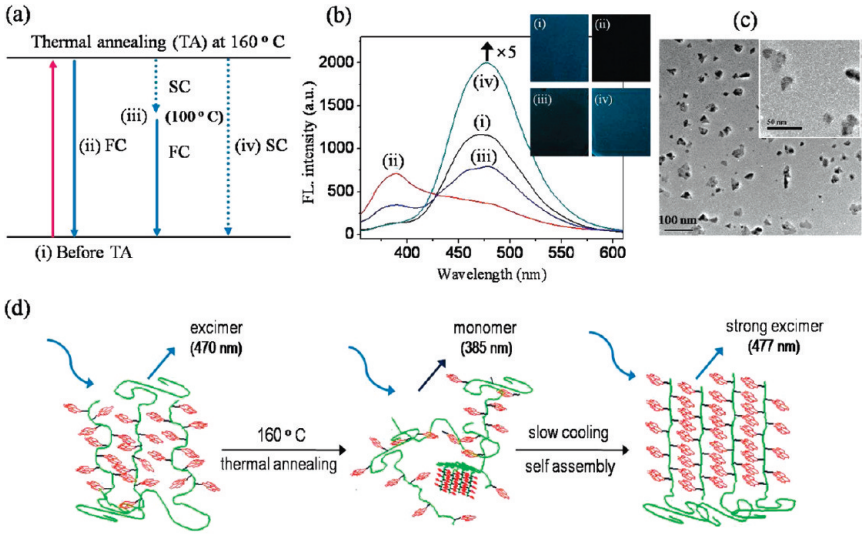

Figure 7. (a) Schematic diagram of the preparation of the four different block copolymer films (i) before thermal annealing, (ii) fast-cooled (FC) using liquid nitrogen after thermal annealing at 160 °C (TA), (iii) slow-cooled (SC) to 100 °C followed by FC to room temperature after TA, and (iv) SC to room temperature after thermal annealing. (b) Fluorescence spectra of the films (i–iv) and photographic images (inset). (c) TEM images of the film (ii) FC using liquid nitrogen after thermal annealing (inset shows a magnified image of pyrene aggregation). (d) Schematic illustration of the generation of well-ordered pyrene structure and mechanism of excimer intensity control by temperature.

temperature (T) (see Figure 6b) correlated well with the Arrhenius relation

$$\Phi_E = 1.57 \exp(-\frac{258}{T}) \quad (1)$$

where Φ_E is the emission quantum yield of the annealed film at the annealing temperature T (given in Kelvin). From this relationship, the activation energy (E_a) for Φ_E change was determined as −2144 J/mol, which must be related to the activation energy for pyrene aggregation that favors excimer formation. The activation energy for the excimer formation of the pyrene block copolymer in this work cannot be directly comparable but significantly lower than that for pyrene (17−36 kJ/mol), under different conditions.[43−45] This indicates that the excimer formation is much easier in the block copolymers due to the self-assembled structure. Since the correlation in Figure 6b is the first example of the activation energy for quantum yield change in pyrene block copolymer film, it can be used as a good precedent for understanding the relationship between quantum efficiency and self-assembly in the film state.

Four different block copolymer films (denoted as i−iv) were prepared using different thermal treatments, as shown in Figure 7a. Interestingly, block copolymer film (ii) (thickness = 43 nm), which was quickly cooled using liquid nitrogen after thermal annealing at 160 °C (TA), showed significantly reduced excimer emission intensity at 470 nm and a considerably increased pyrene monomer emission peak at 385 nm (Figure 7b). In addition, film (iii) (thickness = 40 nm), which was slowly cooled to 100 °C, followed by fast cooling to room temperature after TA, showed intermediate fluorescent properties between the annealed film followed by fast cooling (ii) and annealed film followed by slow cooling (iv) (thickness = 47 nm) (Figure 7b). Figure 7c shows TEM images of the block copolymer film cooled quickly using liquid nitrogen after thermal annealing at 160 °C. Compared to the block copolymer film shown in Figures 5a and 5b), the amount of pyrene aggregation was significantly reduced, as much as 13-fold. These emission spectra and TEM results strongly indicate that most pyrene moieties of block copolymer at 160 °C, which is higher than T_g, exist in a highly flexible polymer chain, allowing segmental motion to free pyrene from aggregation. These pyrene groups are gradually aggregated due to self-assembly when the block copolymer film is slowly cooled to room temperature. The photographic images in Figure 7b inset reveal that the excimer emission intensity of block copolymer is strongly dependent on the nanostructure of the pyrene block copolymer, which is sensitive to temperature.

Table 1. Photophysical Properties of $PMMA_{289}$-*b*-PPY_{65} Films (i−iv) Prepared with THF Solution (5 mg/mL)

	(i) before TA	(ii) TA+FC	(iii) TA+SC(100 ° C) +FC	(iv) TA+SC
I_E/I_M[a]	9.1	0.5	2.3	15.7
Φ[b]	0.68	0.01	0.07	0.89

[a] I_E was obtained at λ_{em} = 477 nm, and I_M was obtained at λ_{em} = 397 nm. [b] Fluorescence quantum yield determined using anthracene in PMMA film (0.24) as a standard.

Table 1 summarizes the photophysical properties, such as the ratio (I_E/I_M) and fluorescence quantum yield, of the four types of the block copolymer films described in Figure 7a. Film (iii), which was slowly cooled to 100 °C, followed by fast cooling to room temperature after thermal annealing, resulted in an intermediate I_E/I_M value of 2.3 between film (ii) and film (iv). The fluorescent quantum yields of pristine

(43) Martinho, J. M. G.; Farinha, J. P.; Berberan-Santos, M. N.; Duhamel, J.; Winnik, M. A. *J. Chem. Phys.* **1992**, *96*, 8143–8149.
(44) Okamoto, M.; Sasaki, M. *J. Phys. Chem.* **1991**, *95*, 6548–6553.
(45) Lemmetyinen, H.; Ikonen, M.; Mikkola, J. *Thin Solid Films* **1991**, *204*, 417–439.

film (i) and annealed film at 160 °C (iv) were 68% and 89%, respectively, as referenced to anthracene in poly(methylmethacrylate) film (24%). On the other hand, the quantum yield of the quickly cooled block copolymer film (ii) using liquid nitrogen after thermal annealing was 1%. This is probably due to the lack of strong excimer emission. The degree of emission enhancement (ξ_F) was determined based on the quantum yields of the films, as referenced to the block copolymer solution. The ξ_F values were 1.5 and 2.0 for the pristine film (i) and annealed film at 160 °C (iv), respectively, indicating that emission was increased to 200% because of the self-assembly of pyrene blocks in the annealed film. On the other hand, the ξ_F value was 0.024 for the fast-cooled film (ii), indicating that 97.6% of the emission in solution is quenched upon fast cooling of the film, because of the lack of pyrene self-assembly.

It has been reported that pyrene shows high oxygen quenching efficiency, which make it suitable for use as an effective optical oxygen sensor.[46] Thus, the fluorescence quenching of the pyrene-based silicon resins was increased rapidly, to ~40% in 12 days.[47] The stability and oxygen quenching efficiency of the block copolymer films **5-i** and **5-iv** were examined under ambient conditions, to compare the effect of normal aging (see Figure S4 in the Supporting Information). The fluorescence quenching of film **5-i** and **5-iv** increases to 20% and 36% after 30 days (37% and 66% after 115 days), respectively. This result indicates that film **5-i** is more stable than film **5-iv** under ambient conditions. Compared to pyrene molecules,[47] the pyrene block copolymer **5** showed a much-lower oxygen quenching efficiency, probably because of the low oxygen permeability of the polymethylmethacrylate (PMMA) chain.[48]

Figure 7d shows a schematic illustration of the generation of well-ordered pyrene structure and mechanism of excimer intensity control by temperature. At 160 °C, pyrenes in the block copolymer exist almost separately, because of the high flexibility of the PMMA polymer chain. Therefore, the fast-cooled block copolymer film (ii) after TA mainly showed pyrene monomer emission at 385 nm, not excimer emission at 477 nm. However, when thermally annealed film at 160 °C was slowly cooled to room temperature, this film showed the strongest excimer emission at 477 nm, because of the strong self-assembly of pyrene moieties. This result may be valuable in the development of self-directing fluorescent nanoassemblies in response to varying organic solvent composition and heat. Further studies are in progress to examine controlling factors for fluorescence as well as self-assembly of the fluorescent diblock copolymers under different external stimuli such as solvent mixture, heat, and light.

Conclusions

Well-defined fluorescent block and random copolymers were synthesized via the atom transfer radical polymerization (ATRP) of methyl methacrylate (MMA) and 1-pyrenemethyl methacrylate (PY). Controlled/living radical polymerization by ATRP enabled precise control of the length and distribution of pyrene units in the polymer chains. By taking advantage of these structurally well-controlled polymers, we quantitatively demonstrated a dramatic increase in excimer emission from block copolymers to detect a nanoscale confinement effect in thin films. Excimer emission from block copolymer was further controlled by thermal annealing, because of the rearrangement of the fluorescent blocks into well-ordered pyrene line structure through enhanced association. Because films of self-assembled diblock copolymers (BCPs) are important for the formation of ordered nanodomains, the fluorescent self-assembling diblock copolymer evaluated in this study could potentially be used to investigate functional BCPs applied to nanophase templates, sensing, and imaging.

Acknowledgment. We acknowledge the financial support of Seoul R&BD Program (10816), and the National Research Foundation (NRF) grant funded by the Korea government (MEST) through the Active Polymer Center for Pattern Integration (No. R11-2007-050-00000-0) as well as the National Science Foundation (DMR 09-69301).

Supporting Information Available: FT-IR of 1-pyrenemethyl methacrylate, polymethylmethacrylate (PMMA), and pyrene-containing block copolymer, $PMMA_{289}$-*b*-PPY_{65}; ^1H NMR of 1-pyrenemethyl methacrylate, pyrene containing random copolymer, P(MMA_{148}-*r*-PY_{20}), and pyrene-containing block copolymer, $PMMA_{289}$-*b*-PY_{65}; schematic illustration of thin and thick $PMMA_{289}$-*b*-PY_{65} film structures; and oxygen quenching for the fluorescence of the block copolymer films over time. This information is available free of charge via the Internet at http://pubs.acs.org/.

(46) (a) Fujiwara, Y.; Amao, Y. *Sens. Actuators B* **2003**, *89*, 187–191. (b) Fujiwara, Y.; Amao, Y. *Sens. Actuators B* **2003**, *89*, 58–61. (c) Ishiji, T.; Kaneko, M. *Analyst* **1995**, *120*, 1633–1638. (d) Fujiwara, Y.; Amao, Y. *Sens. Actuators B* **2002**, *85*, 175–178.
(47) Basu, B. J.; Thirumurugan, A.; Dinesh, A. R.; Anandan, C.; Rajam, K. S. *Sens. Actuators B* **2005**, *104*, 15–22.
(48) Mondal, R.; Shah, B. K.; Neckers, D. C. *J. Photochem. Photobiol., A* **2007**, *192*, 36–40.